INVESTIGATION OF INTERCALATION OF COPPER DOPED TITANIUM DISELENIDE

by

TAYLOR HULBERT

A THESIS

Presented to the Department of Chemistry
and the Robert D. Clark Honors College
in partial fulfillment of the requirements for the degree of
Bachelor of Science

May 2022

An Abstract of the Thesis of

Taylor Hulbert for the degree of Bachelor of Science
in the Department of Chemistry to be taken June 2022

Title: Investigation of Interculation of Coper Doped Titanium Diselenide

Approved: _____*Professor David Johnson*_____
Primary Thesis Advisor

The compound Cu_xTiSe_2 exhibits superconducting behavior due to Cu intercalated into the $TiSe_2$ van der Waals gap. It has been previously shown that Cu can be intercalated into the $TiSe_2$ compounds up to amounts of x = 0.1, with an ideal amount of x = 0.08 for superconductivity. The purpose of this investigation is to intercalate more Cu than previously achieved. An annealing study was carried out by sequentially heating the precursors in 100°C increments on two samples with an aim of x = 0.08 and x = 0.2. The in-plane x-ray diffraction and x-ray reflectivity patterns of the $Cu_{0.20}TiSe_2$ target sample indicate that all of the Cu did not intercalate. Rather, $CuSe_2$ was formed. The data collected for this sample could also indicate the Cu was substituted rather than intercalated. The 8% Cu sample appeared to be fully intercalated into the $TiSe_2$ based on the in-plane x-ray diffraction and x-ray reflectivity patterns.

Acknowledgements

I would like to thank Professor David Johnson who acted as my primary thesis advisor and as a member of my thesis committee. Thank you, Professor Johnson, for letting me work in your research lab at the University of Oregon and for helping me expand my knowledge and experience. I would also like to thank Dr. Angela Rovak who served as my Clarks Honors College thesis advisor and as a member of my thesis committee. I thank Mellie Lemon who was a member of my thesis committee as well as my Graduate Student mentor who I worked with in the David Johnson lab. Thank you Mellie for helping me write and edit this paper as well as teaching me the methods of characterizations.

I also want to thank my fellow undergraduate researcher Sarah Chu for helping me in the lab and for all the moral support you have given me. Thank you for being my chemistry friend throughout my college experience. I also want to thank my other chemistry friend Jack Congel for making me laugh when I was overly stressed out and tired. I also want to thank my mom Lisa Hunt, my step-dad Mark Gaskill, my older brother Carl Hulbert, and my dad Shag Hulbert for listening to all my panicked phone calls about my thesis and college in general. I love you all and thank you for the unending support you have given me throughout my college experience. I truly appreciate how lucky I am to have you all and could not have done this without the support.

Table of Contents

List of Figures

List of Tables

Introduction

Transition metal dichalcogenides (TMDs) consist of a transition metal[1] bonded to chalcogens[2]. Layered TMDs have layers around 6-7 Å which are held together by weak van der Waals forces[3]. (Han et al., 2015). Layered transition metal dichalcogenides are of interest in research pertaining to optoelectronics, lubricants and catalysis. Layered TMDs can act as catalysts for the hydrogen evolution and hydrodesulfurization reactions by providing active sites on the edge of the sheets of the layered materials. (Tedstone et al., 2016). The layered structures of the TMDs and the weak interlayer interactions result in the ability to act as lubricants (Zhao et al., 2013). In the area of optoelectronics layered TMDs with dopants have been seen to elicit superconductivity. In different devices the main cause of deterioration and breakdown of devices is heat that is created due to resistance. Superconductors offer no resistance to electrical current they would not create this waste heat which would save energy and extend the lifetime of the device (The Electrochemical Society, 2016).

These electronic, optical, and magnetic properties of the layer compounds can be altered by adding dopants of transition metals to the structures (Tedstone et al., 2016). The dopant[4] can do one of three things: substitute, intercalate, or form binary compounds. Substitution is more likely if the dopant atom is similarly in size, valence, and coordination to the atom in the lattice. Substitution occurs when an atom within the

[1] Transition metal are chemicals elements that lie in groups 3 through 12 of the period table. (New World Encyclopedia writers, n.d.)
[2] Any of the elements oxygen, sulfur, selenium, and tellurium (group 6 elements) (Merriam-Webster, n.d.)
[3] Van Der Waals forces is the general term used to define the attraction of intermolecular forces between molecules (Libretexts, 2020)
[4] Doping process of incorporating foreign atoms (dopants) into a host lattice

lattice is replaced by the dopant atom. Intercalation occurs when the dopant atom goes between the Van Der Waal gaps of the layers (Tedstone et al., 2016). Figure 1 demonstrates a visual of the difference between substitution and intercalation. Binary compounds can be formed. This can occur when the dopant forms a compound with the chalcogens or with oxygen. The binary compounds can form if intercalation or substitution is not stable or if the binary compounds are easily formed and form quickly. The amount of dopant can alter the characteristics of the material. The synthesis method of layered TMDs can affect the amount of dopant that can be intercalated or substituted into the structure.

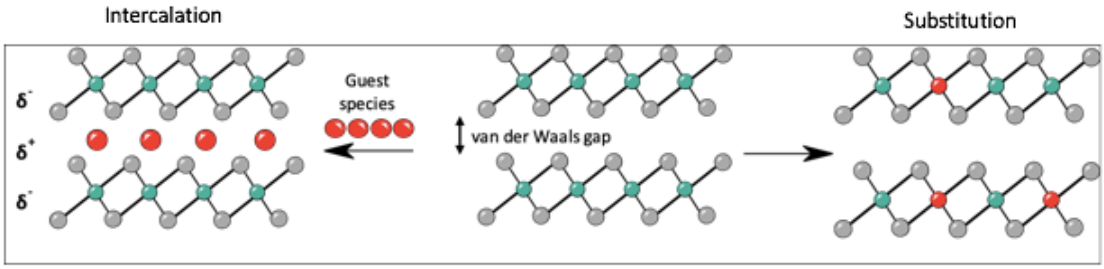

Figure 1. Intercalation vs Substitution is shown above. Where the green represents atoms of metals (Ti for this project), grey is the chalcogen, and red is the dopant. Figure courteous of Mellie Lemon.

New approaches for synthesis of layered TMDs have been developed to produce the heterostructures with controlled thickness and the sequence of layers. These new methods include chemical vapor deposition involving a volatile metal source which involves a monolayer deposition of a metal on a surface then treated at a high temperature with a second regent to form the desired monolayer on substrates (Hamann et al., 2017). The thickness and the sequence of layers are analyzed using methods including Rutherford backscattering, electron probe microanalysis, particle-induced X-ray emission, X-ray fluorescence, and other electron microscopy techniques (Hamann et

al., 2017). These new approaches for synthesis of layered TMDs are what incited this investigation into Cu doped into $TiSe_2$.

Recently, Cu doped $TiSe_2$ has been studied and shown to elicit superconductivity.[5] This superconductivity is the main area of interest for this project. Superconductivity is unable to be reached at room temperatures. High temperature superconductors have been shown to reach superconductivity at 30K and 90K (The Electrochemical Society, 2016). The aim of research in this area is to reach superconductivity at higher temperatures and to find new and different materials that can elicit superconductivity. The increasing amounts of copper caused Cu_xTiSe_2 compounds to reach this superconducting state at higher temperatures (Morosan et al., 2006). The optimal superconducting composition was at x = 0.08 (8%) for the Cu_xTiSe_2 compound (Venkateshwarlu et al., 2012). The optimal amount of copper had a maximum critical temperature of around 4.14K for the transition to superconducting (Hamann et al., 2018). In previous studies the maximum amount of Cu intercalated into the compound was 10% in a single sub-millimeter to millimetric hexagonal plate sample was prepared by the method of mineralization of single crystals that were then heated under vacuum (Levy-Bertrand et al., 2016).

Within this lab, the samples are formed from amorphous precursors layered with the desired elements and nanoarchitecture using modulated elemental reactants (MER). Samples in this study have 20% copper added to the precursor, which is double the amount of copper previous labs were able to intercalate into $TiSe_2$ compounds. The

[5] Superconductivity: the property of materials to conduct direct current without a loss of energy when they reach a critical temperature (U.S. Department of Energy, 2022)

other sample studied had a target of 8% copper; the optimal amount of copper previously intercalated in previous studies.

The 8% Cu sample was chosen to see if the method of MER could be used to successfully intercalate Cu into $TiSe_2$. This amount of Cu has previously been intercalated into $TiSe_2$. This sample is being used to determine if the method of MER could be used to do this. The second sample of 20% Cu was chosen in order to determine if the amount of Cu could be increased passed the previously intercalated amount of 10%. If this amount of Cu can be intercalated this sample can be used to determine if the trend of critical temperature where superconductivity occurs continues with more Cu. Previously critical temperature for Cu_xTiSe_2 reached a maximum at 8% Cu and then decreased as the Cu increased to 10% Cu. Charge density waves are suppressed as the amount of Cu is intercalated into $TiSe_2$ (Morosan et al., 2006). The second sample of 20% of Cu could also be used to investigate this trend of suppression of charge density waves continues as Cu is added. A summary of these trends in superconductivity and charge density waves of Cu_xTiSe_2 is shown below in Figure 2.

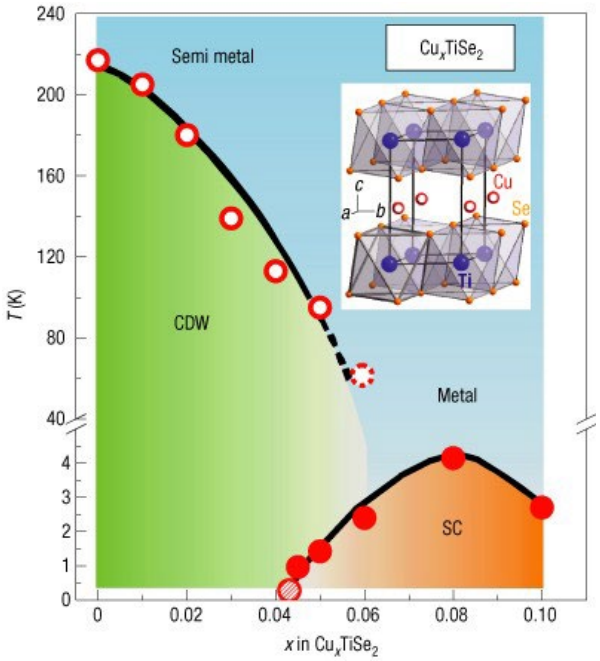

Figure 2. Summary of Trends of Superconductivity and Charge Density Waves for Cu_xTiSe_2. Figure from research Morosan et al. (2006)

The samples will be annealed to promote crystallization of the hexagonal structured $TiSe_2$. The hexagonal unit cell of Cu_xTiSe_2 when it successfully intercalates is shown below in figure 3. The lattice parameters[6] for the unit cell are labeled on the diagram below (a,b, and c).

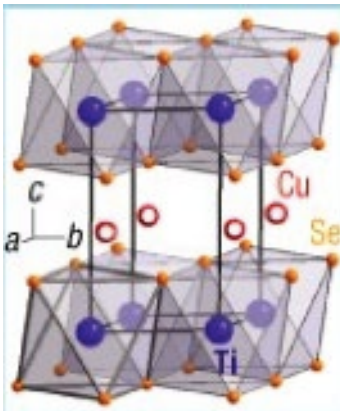

Figure 3. Unit cell of Cu_xTiSe_2 when it intercalates with lattice parameters Figure from research from Morosan et al. (2006)

[6] Lattice parameter is the length between two points on the corners of a unit cell (Libretexts, 2021)

As it is heated then cooled the aim is to have the copper atoms intercalate into the van der Waals gaps of the TMD (Liu et al., 2020). The methods used to characterize the sample and determine if the Cu was able to intercalate into the $TiSe_2$ structure include X-Ray Fluorescence (XRF), specular X-Ray Diffraction (XRD), X-Ray Reflectivity (XRR), and In-plane X-Ray Diffraction.

Methods and Materials

Synthetic Procedures

The elements were deposited onto Si wafers using a custom-built high vacuum physical deposition chamber from elemental sources. The elemental sources were evaporated using electron-beam guns from targets while a Knudson effusion cell evaporated the Se. The sequence of deposition of the intercalation project was Ti|Se|Cu controlled by pneumatic shutters that were between the elemental sources and the spinning substrate.

The elements were deposited in this sequence for enough repeat units to target a film thickness of approximately 300 Å. As the samples were deposited the number of atoms deposited is is monitored using quartz crystal monitors. It is assumed that the number of atoms that hit the crystal rate monitors are proportional to the number of atoms hitting the sample. The samples were made to target specific stoichiometry of the desired compounds (Cordova & Johnson, 2020). The samples are then stored in a nitrogen glovebox to prevent oxidation. Annealing the samples also took place in this nitrogen box on a calibrated hot plate at the desired temperatures. The samples were annealed from 100°C to 400°C or 300°C for 15 minutes at each step in the intercalation project. At 100°C and 200°C the samples were annealed open to the nitrogen atmosphere. At 300°C and 400°C the samples were annealed in a closed container with a Se atmosphere to prevent Se loss as the melting point of Se is around 221°C. The samples were removed from the glovebox for characterization then placed back into the nitrogen glove box for storage.

Characterization

X-ray fluorescence spectroscopy (XRF) was measured using a Rigaku Primus II spectrometer. XRF begins by sending a high energy x-ray at the sample that knocks out a core electron. To stabilize, an electron from a higher orbital will fall into the empty shell. The electron moving from a higher orbital to the core orbital causes the sample to emit a characteristic x-ray that is different for each element. The intensity of the emitted x-ray is measured over the 2θ range appropriate for the energy of the x-ray when diffracted through a crystal with a known d-spacing. The characteristic wavelengths of the elements are known; this information can be used in conjunction with Bragg's law to determine the range of 2θ to measure. The intensity of the emitted x-ray can be converted into atoms/Å^2 for the elements deposited in the sample.

XRR and specular XRD information were collected using Bruker D8 diffractometer with a Cu Kalpha radiation in θ-2θ locked coupled scan mode. XRR was measured over 2θ values of 0-11°. XRR is used to collect information about sample thickness. This information that is calculated from the spacing of the Kiessig fringes and the critical angle. The critical angle is the angle the x-rays start to refract into the sample. Kiessig fringes are used to calculate the thickness of the sample using modified Bragg's Law, which is as follows:

$$\frac{1}{d^2} = \frac{4}{3}\left(\frac{h^2+hk+k^2}{a^2}\right) + \frac{l^2}{c^2}$$

Specular XRD is used to calculate the c-axis lattice parameter with data collected using Smartlab. The scan measured over 2theta values of 5-65°. The data collected from this scan is used to calculate the c-axis lattice parameter using Bragg's law, which is as follows:

$$n\lambda = 2dsin(\theta)$$

The last method used was in-plane XRD. The in-plane scan gives information about the a- and b-axis lattice parameters, which gives information about the phases present in the sample. The in-plane diffraction pattern should match that of hexagonal $TiSe_2$ when totally intercalated with Cu. It is useful to determine if there is another Cu phase when indexing peaks in in-plane patterns.

Results and Discussion

Sample 1B with aim of x = 0.08 for Cu_xTiSe_2.:

Sample 1B was annealed up to 300°C and was analyzed using XRF and specular XRD. In-plane XRD data was not collected on this sample due to an error in the instrument alignment.

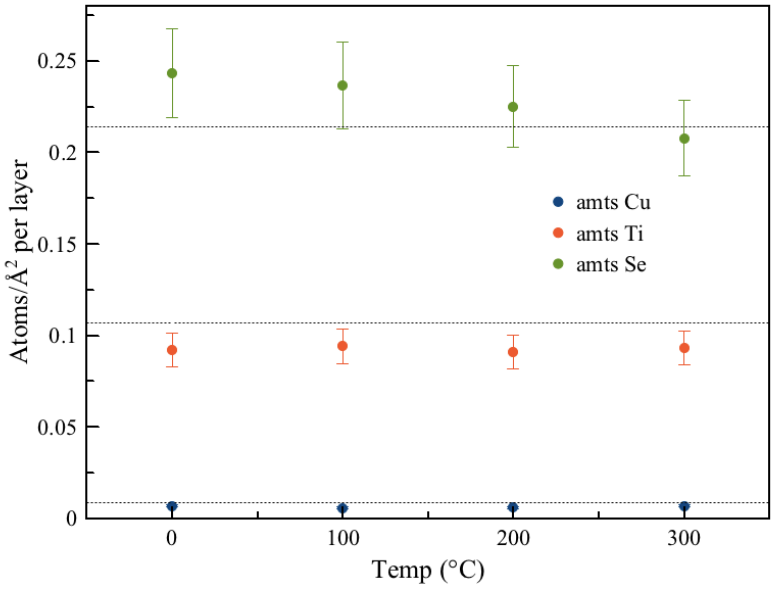

Figure 4. XRF data for $Cu_{0.064}TiSe_{2.2}$

The composition from XRF compared to the targeted composition is summarized in figure 4. The target of this sample was x=0.8; however the actual

composition was $Cu_{0.064}Ti_1Se_{2.2}$ due to less Cu being deposited than targeted. The actual composition was found using the averages of the Atoms•A^{-2}•$Layer^{-1}$ of the metals from Table 1 and the amount of Se after annealing to 300°C.

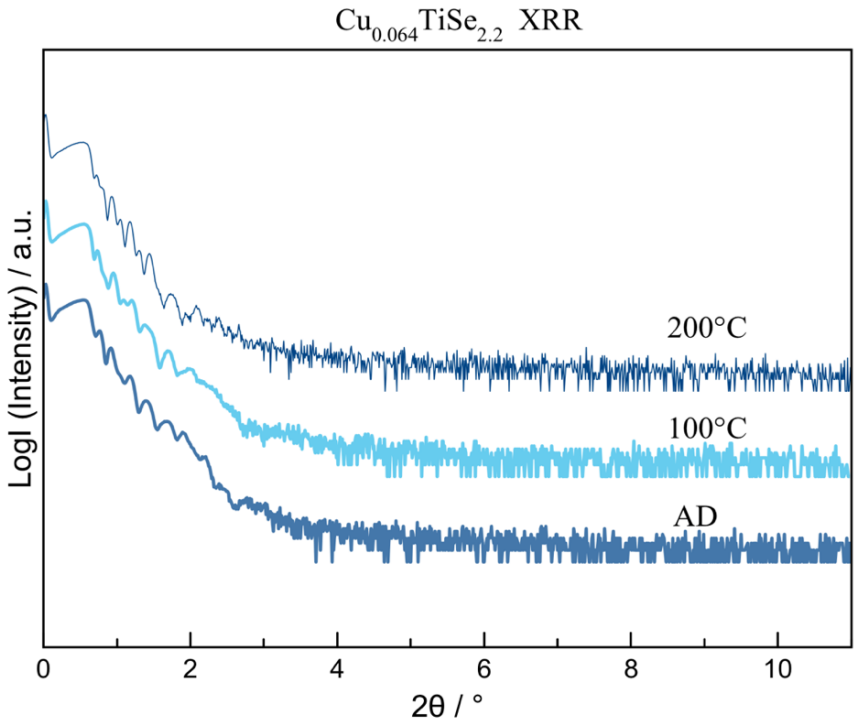

Figure 5. XRR data for $Cu_{0.064}TiSe_{2.2}$

Figure 5 shows the XRR patterns for sample 1B up to 200°C. If this film was wholly homogeneous the scan would show evenly spaced peaks that are smooth however this is not what is seen in the pattern. The period of these peaks (the Kiessig fridges) are related to the thickness of the film. The presence of these fringes are not dependent on the crystallinity of the sample (Miller et al., 2022). The total thickness of the film that was calculated from this data was inconsistent. This could be due to different phases being formed on the film. It appears as if the peaks (especially from the 200°C pattern) are getting narrower and as the temperature is increased it is shifting to the left. From this XRR data it appears to have a layer of another compound (either a

copper oxide or a copper selenide) on the film. It appears to be a layer of another compound because of the two separate 'bumps' seen of the peaks (clearest in 100°C pattern).

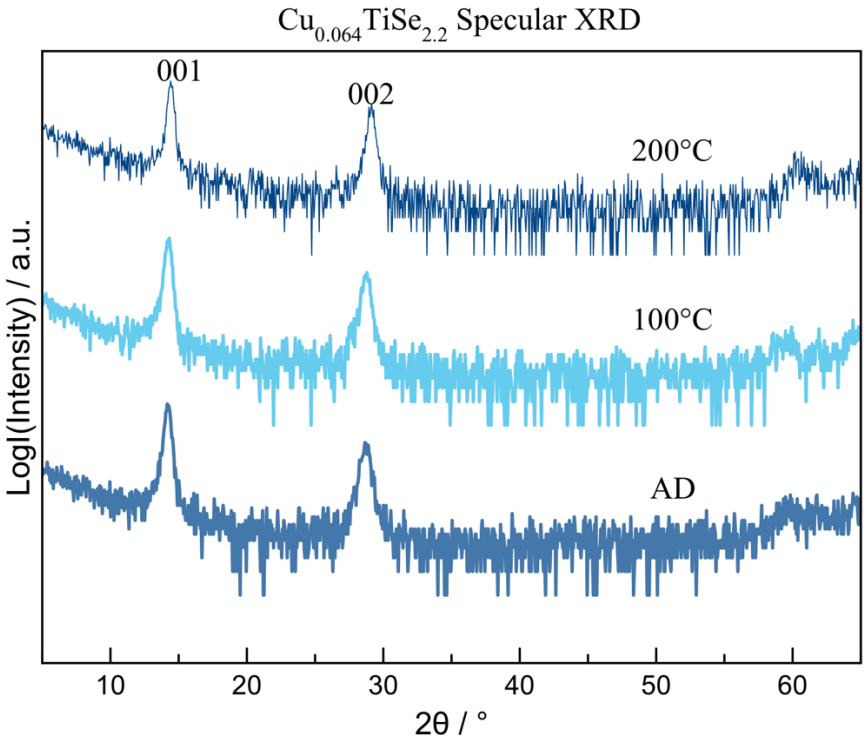

Figure 6. Specular XRD for $Cu_{0.064}TiSe_{2.2}$

The Specular XRD data is shown in Figure 6 and was used to calculate the c-axis lattice parameter for the sample. The calculated c-axis lattice parameters at each temperature are shown in Table 1.

Annealing Temperature	c-axis lattice parameter (Å)
AD	6.22(2)
100°C	6.23(2)
200°C	6.14(1)

Table 1. c-axis Lattice Parameter for $Cu_{0.064}TiSe_{2.2}$

The literature c-axis lattice parameter for $TiSe_2$ is 5.996 Å (FIZ Karlsruhe-Leibniz Institute for Information Infrastructure, 2022). The experimentally calculated c-axis lattice parameter for this sample is around 6 Å, which is near the literature value. The c-axis lattice parameters are also decreasing as the temperature increases which is consistent with the sample crystallizing during the annealing study. If this pattern continues the experimental value will draw nearer to the literature value.

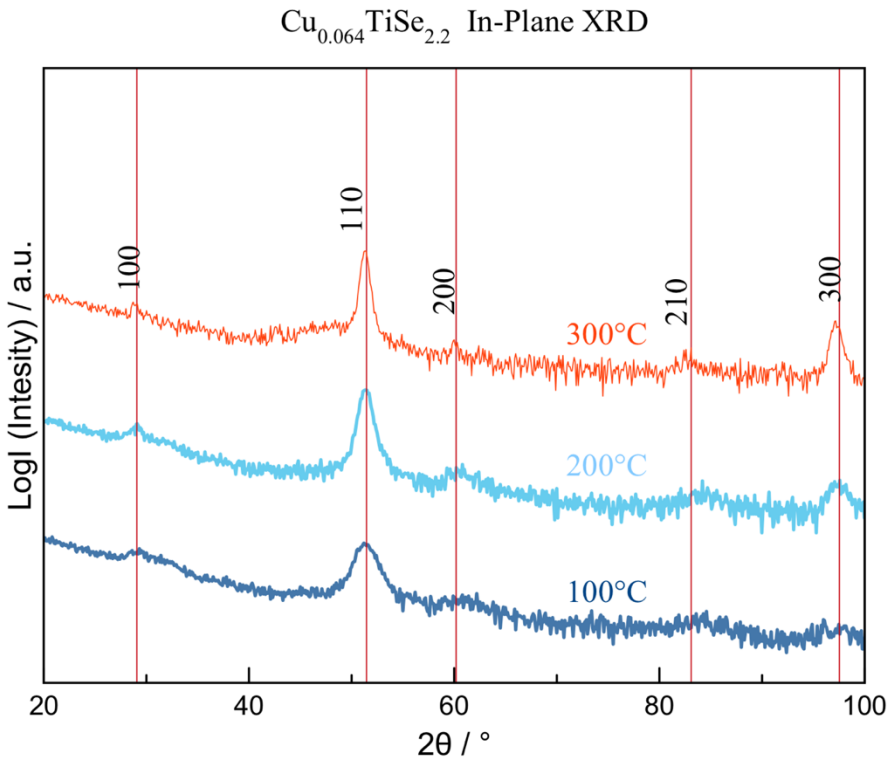

Figure 7. In-Plane XRD Data for $Cu_{0.064}TiSe_{2.2}$ for Sample 1B. Red lines are expected peaks of $TiSe_2$ based on the average a-axis lattice parameter calculated at 200°C

The In-plane pattern (Figure 7) appears to match the expected reflections of hexagonal-structured $TiSe_2$, when indexing the peaks. The reflections seen on the pattern also indicate the sample was aligned on the c-axis, causing the *l* value of the indices to be 0. Based solely on these two temperatures of the annealing study, the Cu has been intercalated; there are no peaks that do not index with the hexagonal $TiSe_2$ compound.

From previous research when Cu is intercalated the lattice parameters calculated are summarized in figure 8 below.

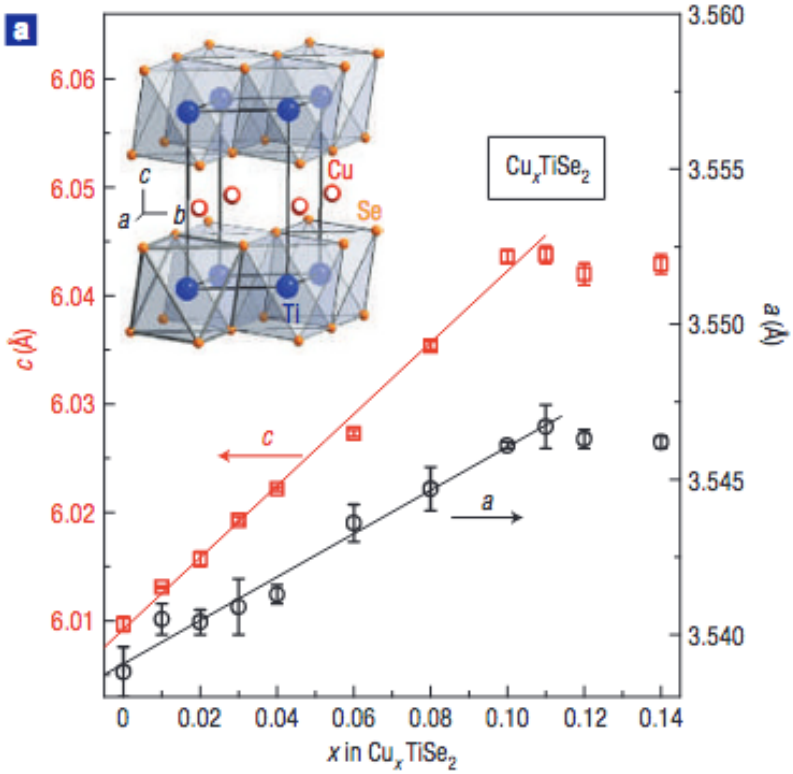

Figure 8. Lattice parameters of Cu_xTiSe_2 when Cu intercalates. Figure from research Morosan et al. (2006)

The a-lattice parameter was used calculated using the peaks from the In-plane data that index to $TiSe_2$. The a-lattice parameter for this sample is around the 3.539 Å

which is the literature value for this parameter (FIZ Karlsruhe-Leibniz Institute for Information Infrastructure, 2022) .The calculated a-axis lattice parameters are listed below in table 2. The lattice parameters for this sample do not change compared to the other sample.

Annealing Temperature	a-axis lattice parameter (Å)
100°C	3.53(7)
200°C	3.58(0)
300°C	3.54(9)

Table 2. a-axis lattice parameters calculated for $Cu_{0.064}TiSe_{2.2}$

Sample 1C with aim x = 0.2 for Cu_xTiSe_2:

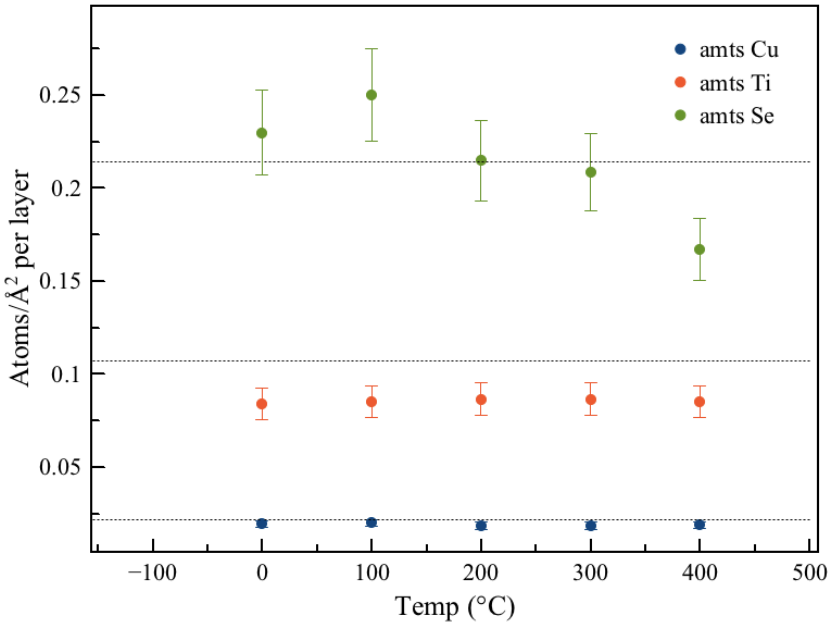

Figure 9. XRF data for $Cu_{0.22}TiSe_{2.4}$

The composition from XRF compared to the targeted composition is summarized in Figure 9. The actual composition of this sample is $Cu_{0.22}TiSe_{2.4}$ found based on the averages for Ti and Cu and Se at 300°C. The amount of Se is decreasing as the annealing temperature is increasing most likely due to the Se evaporating. When annealing to temperatures 300°C and above the sample is annealed in a Se rich

atmosphere to try to limit the amount of Se that is evaporated off during the annealing process.

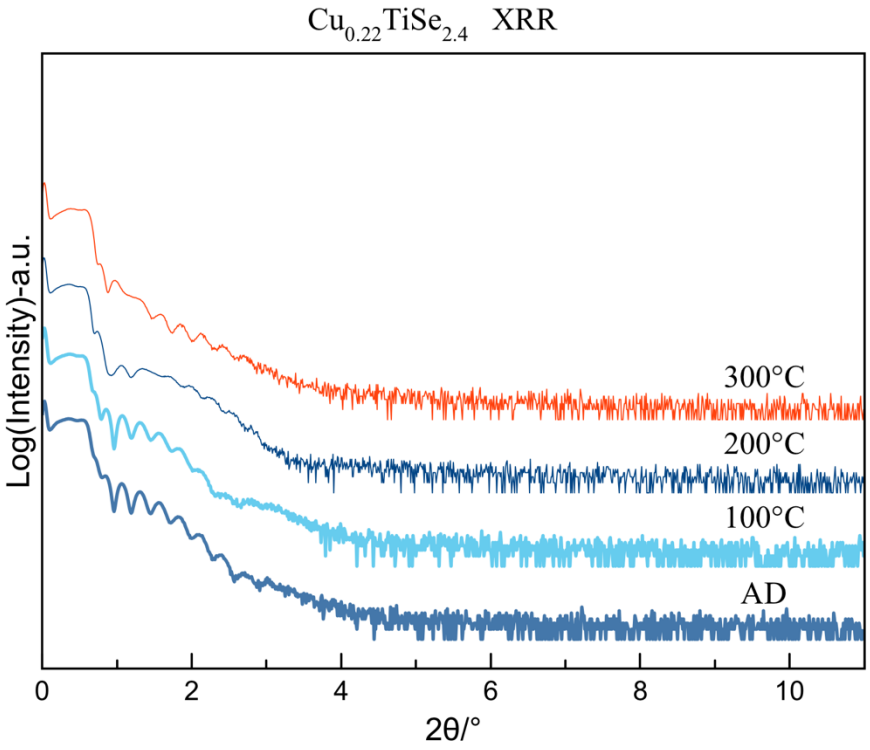

Figure 10. XRR data for $Cu_{0.22}TiSe_{2.4}$ The data for AD-300°C was made using the Bruker

The XRR patterns are shown in Figure 10. The calculated thicknesses of this sample from the XRR patterns were inconsistent and unreliable. This could be due to an interference between two different fringe patterns caused by the formation of a different film on the sample. It is most likely a Cu-Se compound forming, indicating the Cu is not completely intercalating into the $TiSe_2$ compound. The Cu-Se compounds are more likely to be formed as Cu and Se were deposited next to one another. The pattern appear to have two distinct 'bumps' which indicates a separate layer of compound (a copper-selenide). The bumps looks similar to that of the bumps introduced into the Kiessig fringes on figure 11 when an oxide compound forms with the $TiSe_2$. The XRF data for

this compound also indicates a copper selenide compound forming as the Se amount decreases until the excess is in an ~1:2 ratio with copper, in 400°C it goes to a 1:1 ratio. The 400ºC XRR pattern was taken using the Smartlab however it was misaligned with the previous scans made on the Bruker so it was not included in Figure 10.

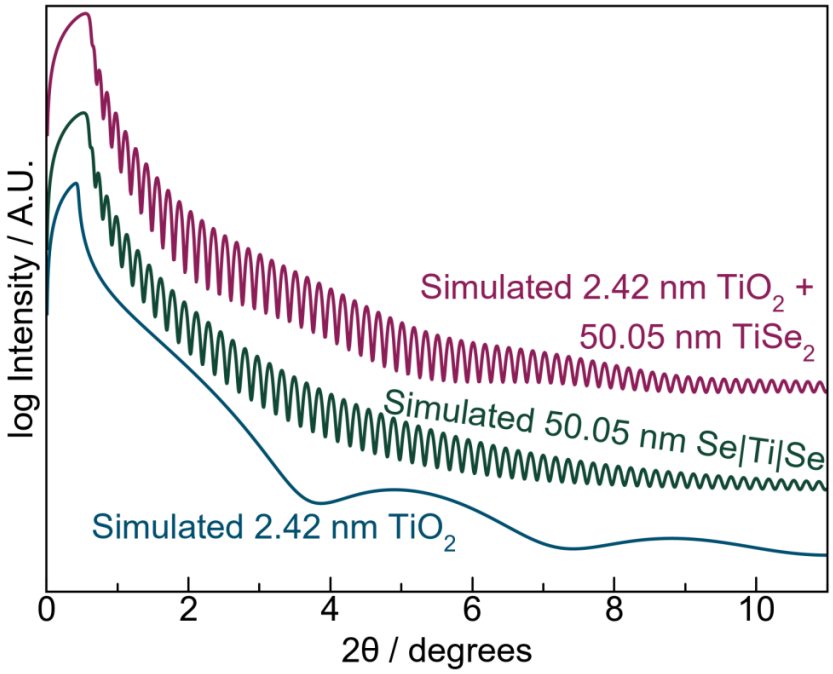

Figure 11. Separate layer of compound effects on XRR pattern. When TiO_2 Is introduced to the $TiSe_2$ shown in red it creates a wave or bump in the fringe patterns. Graph from (Miller et al., 2022).

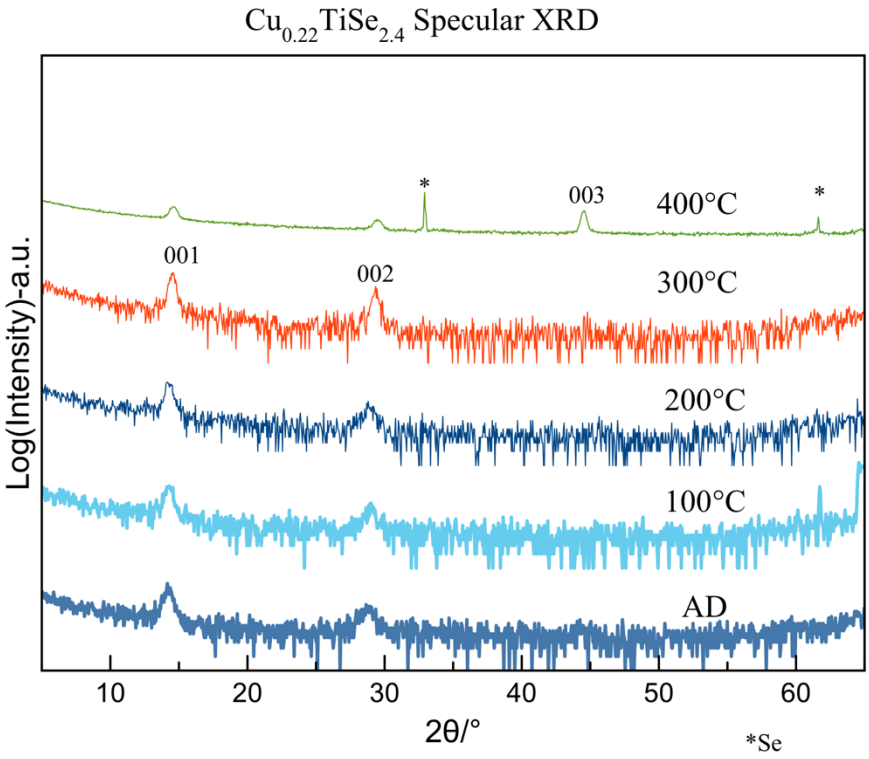

Figure 12. Specular XRD data for $Cu_{0.22}TiSe_{2.4}$. The data for AD-300°C was made using the Bruker while the 400°C spectrum was taken using the Smartlab. Reflections marked with an * are due to the substrate

The specular XRD pattern is shown in Figure 12. The peaks in this spectrum are less intense than that of the previous sample and the peaks are wider. This indicates the sample is less crystalline than the previous sample. The 003 peak appears at 400°C in this spectrum most likely due to the sample becoming more crystalline. The c-axis lattice parameter was calculated using this data from Bragg's law. The c-axis lattice parameters at each temperature are shown in Table 3.

Annealing Temperature	C-axis Parameter (Å)
AD	6.221(2)
100°C	6.183(2)
200°C	6.181(5)
300°C	6.090(7)
400°C	6.063(1)

Table 3. Specular XRD for $Cu_{0.22}Ti_1Se_{2.4}$

The c-axis lattice parameter for this sample was around 6 Å with it decreasing as the temperature increases. The decreasing c-axis parameter indicates that the sample is crystalizing and forming compound(s) during the annealing process. The c-axis lattice parameter is near to the literature value for $TiSe_2$ is 5.996 Å (FIZ Karlsruhe-Leibniz Institute for Information Infrastructure, 2022).

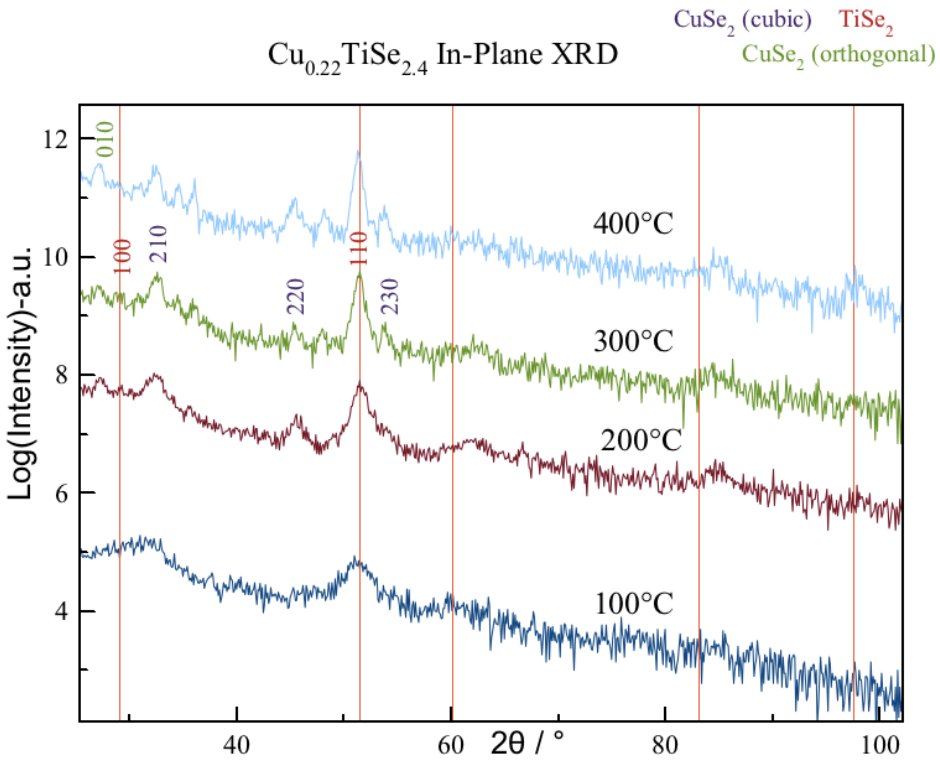

Figure 13. In-Plane XRD Data for $Cu_{0.22}TiSe_{2.4}$ The peaks are indexed for 300°C.

The in-plane XRD patterns are shown in Figure 13. When indexing the peaks of the 200-400°C patterns there are peaks that do not index to a hexagonal $TiSe_2$ compound that are most likely due to a Cu impurity phase. The peaks were then compared to the two different phases of $CuSe_2$. Cubic compound of the $CuSe_2$ is more likely to been seen in the patterns below 300°C while the patterns above 300°C are more likely to have orthogonal $CuSe_2$ compound forming (Thompson et al., 2011).

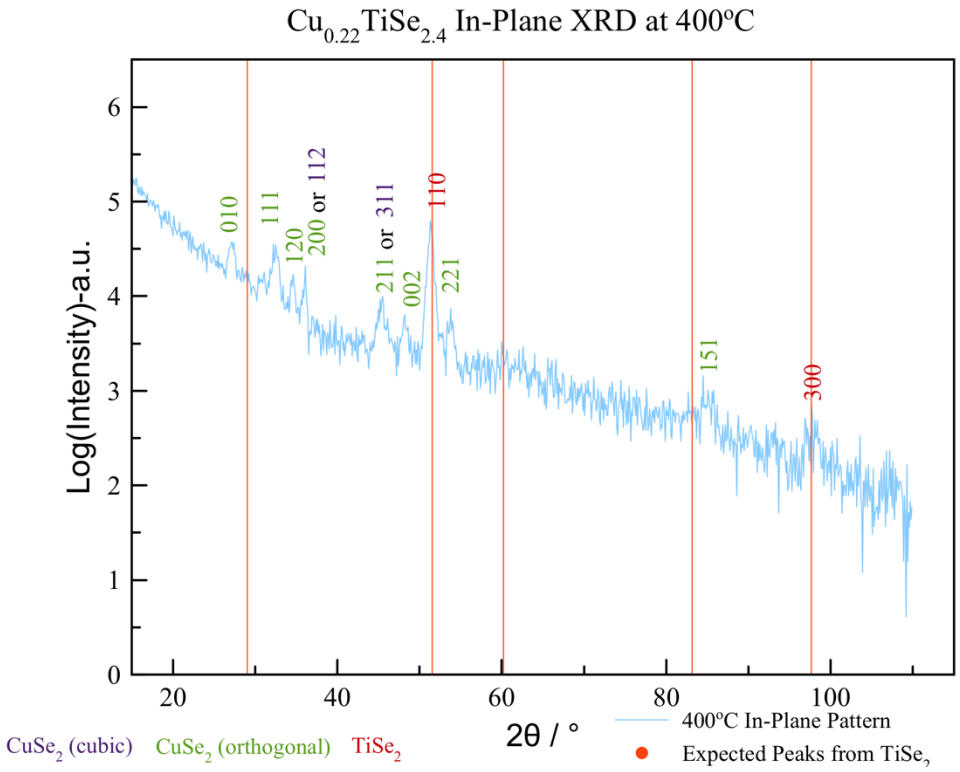

Figure 14. In-Plane XRD for 400°C of $Cu_{0.22}TiSe_{2.4}$ is shown and the peaks are indexed comparing the spectrums to $CuSe_2$ compounds as well as hexagonal $TiSe_2$

The XRD in-plane pattern for 400°C is shown in Figure 14 with indexed peaks. The orthogonal phase of $CuSe_2$ indexes to the peaks seen in the pattern. The peaks around 36° could be either index to the orthogonal $CuSe_2$ reflection of 200 or the cubic $CuSe_2$ 112 reflection. It is most likely the orthogonal phase of the compound as it is

seen at higher temperatures while the cubic version is seen at lower temperatures (Thompson et al., 2011).

The a-lattice parameter for this sample is around the 3.539 Å which is the literature value for this parameter (FIZ Karlsruhe-Leibniz Institute for Information Infrastructure, 2022). The calculated a-axis lattice parameters are listed below in table 4. The calculated values do increase to a maximum of 3.63(7) Å for the sample at 300°C.

Annealing Temperature	a-axis lattice parameter (Å)
100°C	3.56(6)
200°C	3.51(7)
300°C	3.63(7)
400°C	3.55(9)

Table 4. a-axis lattice parameters calculated for $Cu_{0.22}TiSe_{2.4}$

The values for a-axis lattice parameters for this sample are higher than that of the intercalated copper sample shown in figure 8. The values in figure 8 for these axis parameters plateau around 3.548 (Å) while the values calculated for this sample are all (except for 200°C) higher than this value. The a-axis lattice parameter does not match that of an intercalated sample for Cu doped $TiSe_2$.

Conclusion

The sample 1B with the aim of x = 0.08 for Cu_xTiSe_2 has been annealed up to 300ºC. This sample's composition is $Cu_{0.064}Ti_1Se_{2.2}$. The current in-plane XRD of the 100-200ºC appears to have the Cu fully intercalated into hexagonal $TiSe_2$, as the peaks index to this phase of $TiSe_2$ and no other peaks indicating another phase are seen on the patterns. The c-axis lattice parameters calculated for the current temperature is near the literature value, however the XRR patterns appear to have some interference that hinder

the calculation of the thickness. The annealing study for this compound needs to be finished for this sample to see if the Cu-Se compounds form as the temperature increases or if the patterns support the idea of the Cu fully intercalating into the hexagonal $TiSe_2$ structure.

The sample 1C with the aim of x = 0.2 for Cu_xTiSe_2 data indicates that the full amount of Cu did not intercalate into the $TiSe_2$. The composition was actually $Cu_{0.22}Ti_1Se_{2.4}$. The in-plane XRD data has peaks that did not index to the hexagonal phase of $TiSe_2$. These peaks indexed to either the cubic phase of $CuSe_2$ or orthogonal phase of $CuSe_2$, indicating these compounds form during the annealing study. The a-axis parameters were higher than the expected values for intercalated Cu_xTiSe_2. The increase of the a-axis lattice parameter could indicate that the Cu substituted into the $TiSe_2$. If the Cu substituted the in-plane XRD would have peaks that do not index to $TiSe_2$. This also would explain why the c-axis lattice parameter decreases as the annealing study continued. This theory of the Cu substituting does not explain the XRR patterns. The XRR pattern could be due to interference between different fringe patterns due to different compounds of Cu-Se forming a layer on the sample.

Data collected supports the idea that Cu is able to be intercalated into the $TiSe_2$ structure at amounts around 6% using the method of modulated elemental reactants (MER). However, at amounts of 19% Cu it appears the Cu was not be intercalated into the $TiSe_2$ compound even using MER. The data collected could indicate the sample with 19% Cu had the Cu substitute rather than intercalate. The Cu-Se compounds could have required less energy to form that it takes for the Cu to intercalate.

Next steps

Possible next steps for this project might include the following.

The samples might be remade without depositing Cu and Se next to each other. The deposition would have repeating layers of Ti|Se|Ti|Cu to try to prevent the Cu and Se from forming compounds.

Another avenue for this project might be to make new samples with less Cu. The attempt to intercalate 20% of Cu was an attempt to double the previous amount other methods have successfully intercalated. The MER method was able to intercalate Cu at lower amounts so it may be beneficial to attempt to intercalate more Cu than previous attempts but less than double. A sample of 15%, 13%, and/or 17% Cu would be options to prove that MER is able to intercalate more Cu than other methods.

After the annealing study is completed on the 6% Cu sample (1B) the electrical properties of the samples could be measured to determine how the amount of Cu affects the superconductivity of the $TiSe_2$ compound when prepared with MER. If the amount of Cu is able to be intercalated, then the next aim would be to attempt to reduce the thickness of the Cu_xTiSe samples to reach the 2D limit and to measure the electronic properties of the compounds. The purpose of this is to measure how the increasing amount of intercalated Cu and the decreasing thickness of the sample would affect the CDW and superconducting states. This is because it has been previously seen to show different properties than their bulk counterparts (Kolobov et al, 2016).

Bibliography

Cordova, D. L. M., & Johnson, D. C. (2020). Synthesis of Metastable Inorganic Solids with Extended Structures. *ChemPhysChem*, *21*(13), 1345–1368. https://doi.org/10.1002/cphc.202000199

FIZ Karlsruhe-Leibniz Institute for Information Infrastructure. (2022). *ICSD* -. ICSD. https://icsd.fizkarlsruhe.de/index.xhtml;jsessionid=DB42C469344BD5C1BD78936DDF3E205D

Hamann, D. M., Bardgett, D., Cordova, D. L. M., Maynard, L. A., Hadland, E. C., Lygo, A. C., Wood, S. R., Esters, M., & Johnson, D. C. (2018). Sub-Monolayer Accuracy in Determining the Number of Atoms per Unit Area in Ultrathin Films Using X-ray Fluorescence. *Chemistry of Materials*, *30*(18), 6209–6216. https://doi.org/10.1021/acs.chemmater.8b02591

Hamann, D. M., Hadland, E. C., & Johnson, D. C. (2017). Heterostructures containing dichalcogenides-new materials with predictable nanoarchitectures and novel emergent properties. *Semiconductor Science and Technology*, *32*(9), 093004. https://doi.org/10.1088/1361-6641/aa7785

Han, S. A., Bhatia, R., & Kim, S. W. (2015). Synthesis, properties and potential applications of two-dimensional transition metal dichalcogenides. *Nano Convergence*, *2*(1). https://doi.org/10.1186/s40580-015-0048-4

Kolobov, & Tominaga, Junji. (2016). *Two-dimensional transition-metal dichalcogenides.* Springer.

Levy-Bertrand, F., Michon, B., Marcus, J., Marcenat, C., Kačmarčík, J., Klein, T., & Cercellier, H. (2016). Puzzling evidence for surface superconductivity in the layered dichalcogenide Cu<mml:math altimg="si1.gif" overflow="scroll" xmlns:xocs="http://www.elsevier.com/xml/xocs/dtd" xmlns:xs="http://www.w3.org/2001/XMLSchema" xmlns:xsi="http://www.w3.org/2001/XMLSchema-instance" xmlns="http://www.elsevier.com/xml/ja/dtd" xmlns:ja="http://www.elsevier.com/xml/ja/dtd" xmlns:mml="http://www.w3.org/1998/Math/MathML" xmlns:tb="http://www.elsevier.com/xml/common/table/dtd" xmlns:sb="http://www.elsevier.com/xml/common/struct-bib/dtd" xmlns:ce="http://www.elsevier.com/xml/common/dtd" xmlns:xlink="http://www.w3.org/1999/xlink" xmlns:cals="http://www.elsevier.com/xml/common/cals/dtd" xmlns:sa="http://www.elsevier.com/xml/common/struct-aff/dtd"><mml:msub><mml:mrow/><mml:mrow><mml:mn>10</mml:mn><mml:mo>%</mml:mo></mml:mrow></mml:msub></mml:math>TiSe2. *Physica C: Superconductivity and Its Applications*, *523*, 19–22. https://doi.org/10.1016/j.physc.2016.02.004

Libretexts. (2020, August 15). *Van der Waals Forces*. Chemistry LibreTexts. https://chem.libretexts.org/Bookshelves/Physical_and_Theoretical_Chemistry_Textbook_Maps/Supplemental_Modules_(Physical_and_Theoretical_Chemistry)/Physical_Properties_of_Matter/Atomic_and_Molecular_Properties/Intermolecular_Forces/Van_der_Waals_Forces

Libretexts. (2021, March 21). *7.1: Crystal Structure*. Chemistry LibreTexts. https://chem.libretexts.org/Bookshelves/Analytical_Chemistry/Physical_Methods_in_Chemistry_and_Nano_Science_(Barron)/07%3A_Molecular_and_Solid_State_Structure/7.01%3A_Crystal_Structure

Liu, X. C., Zhao, S., Sun, X., Deng, L., Zou, X., Hu, Y., Wang, Y. X., Chu, C. W., Li, J., Wu, J., Ke, F. S., & Ajayan, P. M. (2020). Spontaneous self-intercalation of copper atoms into transition metal dichalcogenides. *Science Advances*, *6*(7). https://doi.org/10.1126/sciadv.aay4092

Merriam-Webster. (n.d.). *chalcogen*. The Merriam-Webster.Com Dictionary. Retrieved 2022, from https://www.merriam-webster.com/dictionary/chalcogen

Miller, A. M., Lemon, M., Choffel, M. A., Rich, S. R., Harvel, F., & Johnson, D. C. (2022). Extracting information from X-ray diffraction patterns containing Laue oscillations. *Zeitschrift Für Naturforschung B*, *0*(0). https://doi.org/10.1515/znb-2022-0020

Mora-Fonz, D., Schön, J. C., Prehl, J., Woodley, S. M., Catlow, C. R. A., Shluger, A. L., & Sokol, A. A. (2020). Real and virtual polymorphism of titanium selenide with robust interatomic potentials. *Journal of Materials Chemistry A*, *8*(28), 14054–14061. https://doi.org/10.1039/d0ta03667f

Morosan, E., Zandbergen, H. W., Dennis, B. S., Bos, J. W. G., Onose, Y., Klimczuk, T., Ramirez, A. P., Ong, N. P., & Cava, R. J. (2006). Superconductivity in CuxTiSe2. *Nature Physics*, *2*(8), 544–550. https://doi.org/10.1038/nphys360

New World Encyclopedia writers. (n.d.). *Transition metal - New World Encyclopedia*. New World Encyclopedia. https://www.newworldencyclopedia.org/entry/Transition_metal

Tedstone, A. A., Lewis, D. J., & O'Brien, P. (2016). Synthesis, Properties, and Applications of Transition Metal-Doped Layered Transition Metal Dichalcogenides. *Chemistry of Materials*, *28*(7), 1965–1974. https://doi.org/10.1021/acs.chemmater.6b00430

The Electrochemical Society. (2016, July 13). *Global Superconductor Applications*. ECS. https://www.electrochem.org/superconductors

Thompson, J. O., Anderson, M. D., Ngai, T., Allen, T., & Johnson, D. C. (2011). Nucleation and growth kinetics of co-deposited copper and selenium precursors to form metastable copper selenides. *Journal of Alloys and Compounds*, *509*(40), 9631–9637. https://doi.org/10.1016/j.jallcom.2011.07.042

U.S. Department of Energy. (2022). *DOE Explains. . .Superconductivity*. Energy.Gov. https://www.energy.gov/science/doe-explainssuperconductivity

Venkateshwarlu, D., Samatham, S. S., Gangrade, M., & Ganesan, V. (2012). Superconductivity in $Cu_{0.08}TiSe_2$. *AIP Conference Proceedings*. https://doi.org/10.1063/1.4710287

Zhao, Y., Luo, X., Li, H., Zhang, J., Araujo, P. T., Gan, C. K., Wu, J., Zhang, H., Quek, S. Y., Dresselhaus, M. S., & Xiong, Q. (2013). Interlayer Breathing and Shear Modes in Few-Trilayer MoS_2 and WSe_2. *Nano Letters*, *13*(3), 1007–1015. https://doi.org/10.1021/nl304169w